Near-Body Mesh Adaptation for Transitional Flows using OVERFLOW

Balaji Venkatachari
Analytical Mechanics Associates Inc., Hampton VA

Michael Donello, Joseph Derlaga, and Meelan Choudhari
NASA Langley Research Center, Hampton, VA

July 17, 2024
Mesh Generation/Adaptation II
ICCFD12, Kobe, Japan

ANALYTICAL MECHANICS ASSOCIATES

NATO and AIAA Transition Modeling Workshops: Sample Results

Langtry-Menter Model

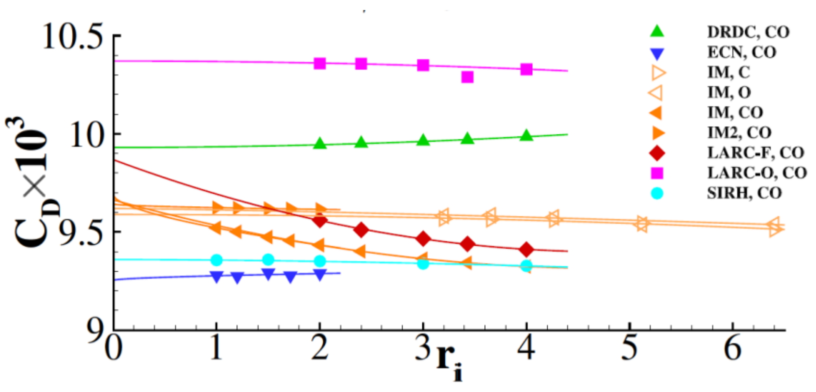

Eppler 387 Airfoil (AoA = 1 deg; Re_c = 300,000)

NATO AVT-313 Workshop[1]

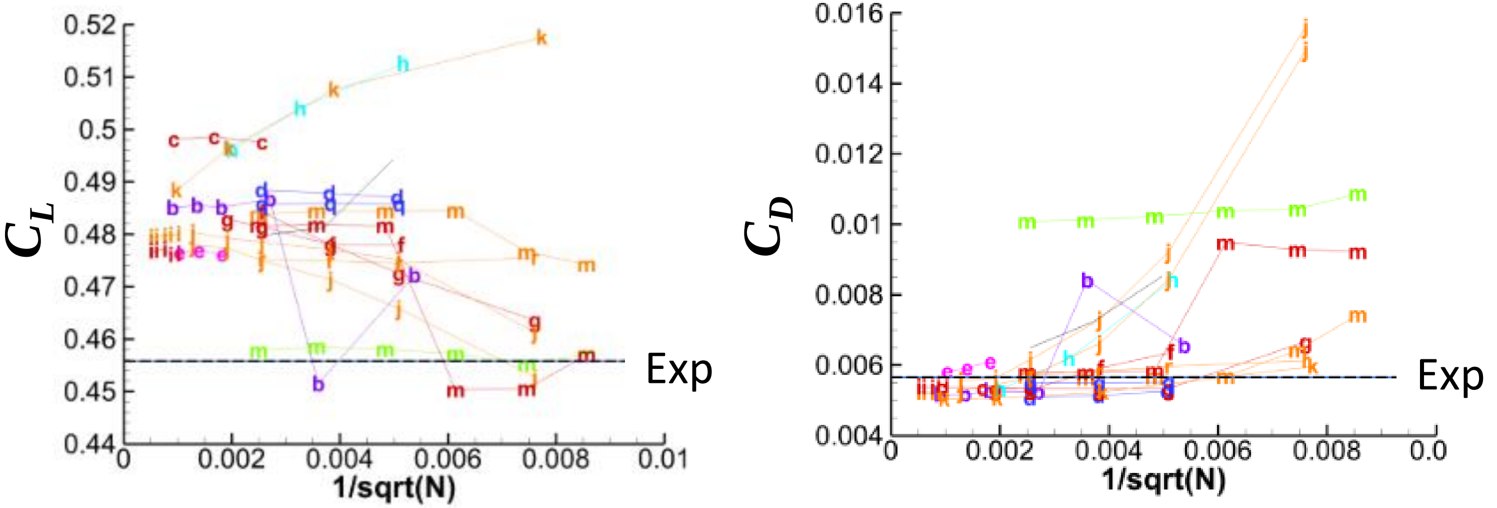

NLF-0415 Airfoil (AoA = 0 deg; Re_c = 4,000,000)

AIAA 1st Transition Modeling and Prediction Workshop[2]

- Significant scatter amongst results from different codes as the grid was refined
  - Inadequate refinement of grids? Grid convergence properties strongly dependent on the solvers.
  - Inconsistencies in implementing the details of the transition model?

1. https://web.tecnico.ulisboa.pt/ist12278/Workshop_AVT_313_2D_cases/Workshop_AVT_313_2D_cases.htm
2. https://transitionmodeling.larc.nasa.gov/workshop_i/

Verification of Transition Model: Grid Resolution Requirements

Mesh Level	No. of points in chordwise direction	No. of points in wall-normal direction	No. of points in wake-cut
Mesh 1	353	49	49
Mesh 2	529	73	73
Mesh 3	705	97	97
Mesh 4	1057	145	145
Mesh 5	1409	193	193
Mesh 6	2113	289	289
Mesh 7	2817	385	385
Mesh 8	4225	577	577
Mesh 9	5633	769	769
Mesh 10	8449	1153	1153

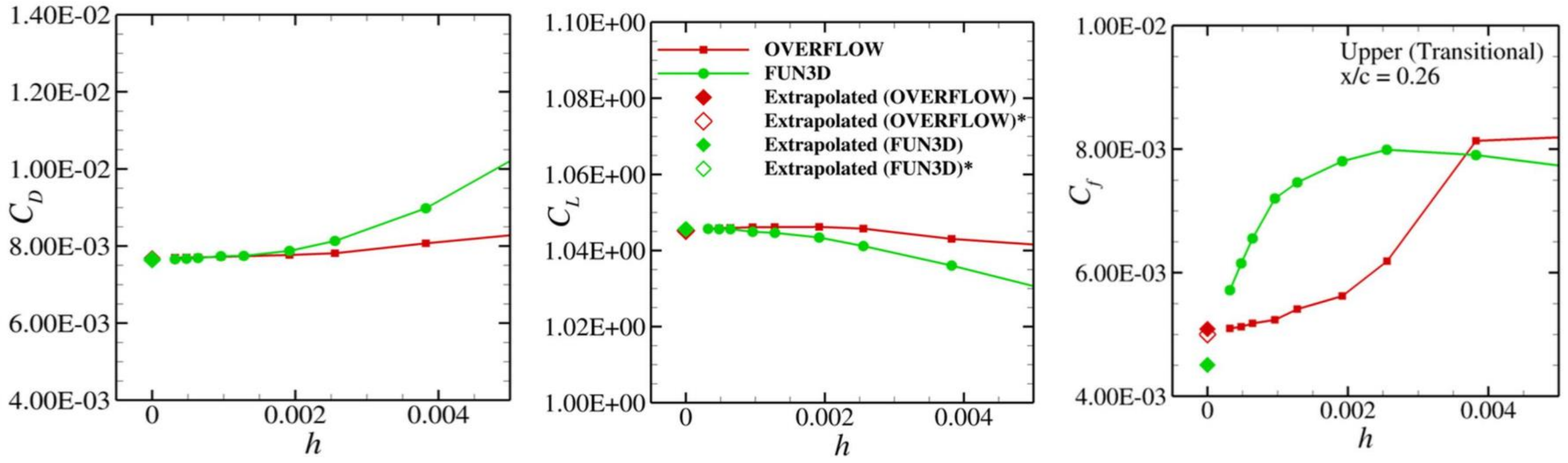

Langtry-Menter Model: NLF-0415 Airfoil (AoA = 5 deg; $Re_c = 4 \times 10^6$)

- Satisfactory grid convergence could be achieved for 2D canonical flows[1]
  - Required mesh counts of O(10^7) for demonstrating asymptotic convergence of point quantities
  - Further efforts are necessary to reduce the mesh sizes to enable 3D computations

1. Venkatachari, B. S., Denison, M., Mysore, P. V., Hildebrand, N., and Choudhari, M. M., "Verification of the γ-Reθt Transition Model in OVERFLOW and FUN3D," *AIAA Journal of Aircraft*, Vol. 61, No.2, March-April 2024. https://doi.org/10.2514/1.C037445

Outline

- Objectives
- About the LM Model and OVERFLOW
- Near-body mesh adaptation sensor/mechanics
- Test cases: Flat Plate , S809, NLR-7301 (Multiple transition scenarios)
- Summary and Future Work

Objectives

Long-term objectives

- Accurate prediction of viscous flows with laminar-to-turbulent boundary-layer transition (CFD 2030)
- Efficiently accelerate the grid convergence of RANS-based transition models by improving the mesh resolution in critical parts of the flow field
- Identify the best practices related to grid design for RANS-based transition model computations by CFD practitioners

This work

- Using automated isotropic **near-body mesh adaptation** capability in **OVERFLOW** to **achieve grid-insensitive solutions with reduced mesh counts for the Langtry-Menter (LM) transition model**
  - Mesh adaptation capability in OVERFLOW has not been studied earlier in the context of flows undergoing transition (and its effect on relevant flow metrics)
  - Need for transition-specific error metrics for mesh adaptation
- Assessment of benefits from the mesh adaptation approach: flow conditions involving multiple transition scenarios

Status: Exploratory work and results should be considered as work in progress

Prior Related Work

Mesh Adaptation

1. Recognizing areas where additional resolution is needed [Roy, 2009]
   - Feature-based, Solution error estimation, Goal-based (adjoints)
2. A mechanism to alter the mesh [Baker, 1997]

- Increased use of Mesh adaptation for turbulent flow computations [AIAA high-lift workshops] [Park et al., 2016]

Mesh adaptation work for RANS-based computations of flows undergoing transition

1) Hildebrand et al. (2024) - LM model
   - Zonal, structured-mesh refinement strategies, Mach-Hessian-based unstructured grid adaptation
   - Importance of streamwise vs wall-normal resolution

2) Gosin et al. (2024) – Amplification Factor Transport (AFT) model
   - Output-based (adjoint) mesh adaptation (modification of AFT model needed: C^0-continuous terms)
   - Local shape-factor in model inhibited convergence and the mesh adaptation process

The Langtry-Menter Model

Solves two additional scalar equations, implemented upon SST model (2003 version)[1]

- Correlation-based: Dependent on local pressure gradient and turbulence disturbance levels (*Tu*)
- Transport equation[2] for intermittency ($\boldsymbol{\gamma}$) and transition momentum-thickness Reynolds number ($\boldsymbol{Re_{\theta t}}$)
- Can model natural, bypass and separation-induced transition scenarios

$$\frac{\partial(\rho k)}{\partial t}+\frac{\partial(\rho u_j k)}{\partial x_j}=\gamma_{eff}\,P_{\lim}-\min(\max(\gamma_{eff},\,0.1),1.0)\beta^*\rho\omega k+\frac{\partial}{\partial x_j}\left[(\mu+\sigma_k\mu_t)\frac{\partial k}{\partial x_j}\right], \quad (1)$$

$$\frac{\partial(\rho\omega)}{\partial t}+\frac{\partial(\rho u_j\omega)}{\partial x_j}=\frac{\alpha}{\nu_t}P_{\lim}-\beta\rho\omega^2+\frac{\partial}{\partial x_j}\left[(\mu+\sigma_\omega\mu_t)\frac{\partial\omega}{\partial x_j}\right]+2(1-F_1)\frac{\rho\sigma_{\omega 2}}{\omega}\frac{\partial k}{\partial x_j}\frac{\partial\omega}{\partial x_j}, \quad (2)$$

SST (equations 1–2)

$$\frac{\partial(\rho\gamma)}{\partial t}+\frac{\partial(\rho U_j\gamma)}{\partial x_j}=P_\gamma-E_\gamma+\frac{\partial}{\partial x_j}\left[\left(\mu+\frac{\mu_t}{\sigma_j}\right)\frac{\partial\gamma}{\partial x_j}\right], \quad (3)$$

$$\frac{\partial(\rho\widetilde{Re}_{\theta t})}{\partial t}+\frac{\partial(\rho U_j\widetilde{Re}_{\theta t})}{\partial x_j}=P_{\theta t}+\frac{\partial}{\partial x_j}\left[\sigma_{\theta t}(\mu+\mu_t)\frac{\partial\widetilde{Re}_{\theta t}}{\partial x_j}\right]. \quad (4)$$

1. Menter, F. R., Kuntz, M., and Langtry, R., "Ten Years of Industrial Experience with the SST Turbulence Model," *Turbulence, Heat and Mass Transfer*, Vol. 4 (1), 2003, pp. 625-632.
2. Langtry, R. B., and Menter, F. R., "Correlation-Based Transition Modeling for Unstructured Parallelized Computational Fluid Dynamics Codes," *AIAA Journal*, Vol. 47, No. 12, 2009, pp.2894–2906.

NASA CFD Solver: OVERFLOW

OVERFLOW (2.4c)[1]

- Implicit structured overset grid Navier-Stokes solver
- Successive symmetric overrelaxation (SSOR) implicit solution algorithm
- Third-order accurate discretization (convective terms), second-order accurate (gradients)
- RANS-based transition models (release version): LM2009/LM2015 (SST); AFT 2017b/2019b (SA); Medida-Baeder (SA)
- Near-body[2] and off-body[3] overset mesh adaptation capability (isotropic adaptation based on sensor function/error-estimate)
  - Heuristic approach and has limited applicability
  - Easier than the more powerful, but difficult to implement, adjoint-driven approach
  - Requires fringe points that expand refinement beyond marked regions

Mesh Adaptation Mechanics

1) Sensor function translated into marker function (regions in need of refinement/coarsening and by how much)
2) Parametric cubic interpolation to generate newer grid system using the baseline mesh geometry
3) Interpolation of flow from old grid system to the new system

1. Nichols, R. H, and Buning, P. G., “User’s Manual for OVERFLOW 2.3, Version 2.3,” NASA Langley Research Center, Hampton, VA, Oct 2019.
2. Buning, P. G. and Pulliam, T.H., “Near-Body Grid Adaptation for Overset Grids,” AIAA Paper 2016-3326, 2016. https://doi.org/10.2514/6.2016-3326
3. Meakin, R. L., “An Efficient Means of Adaptive Refinement Within Systems of Overset Grids,” AIAA Paper 95-1722, 1995. https://doi.org/10.2514/6.1995-1722

Sensor Function for Adaptation

- Default sensor function in OVERFLOW : undivided difference of second-difference of the primary flow variables
  - Undivided difference: computed differences are not being divided by the appropriate spatial difference term (say Δx^2 for the second difference)
  - Provided the solution is smooth, the undivided difference tends to decay as the grid is refined, unlike a gradient or Laplacian
- Did not provide accurate results with RANS-based transition models and in fully-turbulent region for boundary-layer type flows (mesh adapted in non-critical areas)
- Need for transition model specific sensors (intermittency γ ?, any other ?)
  - Intermittency, while useful in the laminar region and transition zones, did not help in fully turbulent regions

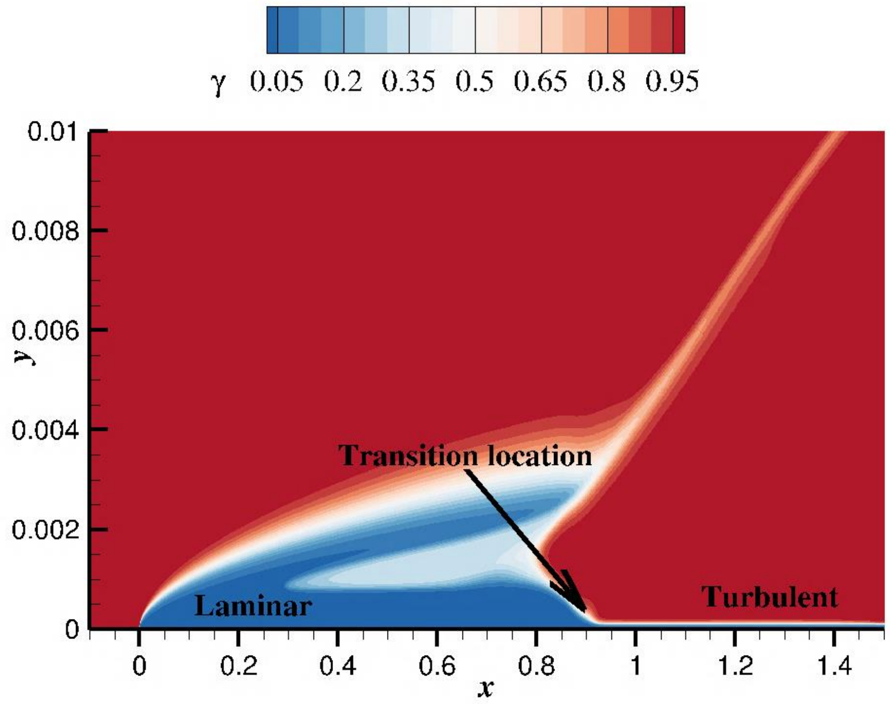

Sensor Function for Adaptation (contd.)

- Transition model specific sensor
  - Vorticity-based Reynolds number: surrogate to estimate momentum thickness and evaluate transition-onset criteria (LM/AFT/ γ models)
  - Sensor-based on undivided vorticity magnitude augmented with blending function from the LM model

$$S_1 = \left(\omega_x^2 + \omega_y^2 + \omega_z^2\right)^{1/2},$$

$\omega_x, \omega_y,$ and ω_z are the three vorticity components computed using central differencing(undivided).

$$\omega_z = (w_{j+1}\text{-}w_{j-1})/(2) - (v_{k+1}\text{-}v_{k-1})/(2)$$

$$F_{\theta t} = min\left(max\left(F_{wake} \cdot e^{-(y/\delta)^4}, 1.0 - \left(\frac{\gamma - 1/c_{e2}}{1.0 - 1/c_{e2}}\right)^2\right), 1.0\right)$$

$$F_{wake} = e^{-\left(\left(\rho\omega y^2/\mu\right)/1E+5\right)^2}; \; c_{e2} = 50.0$$

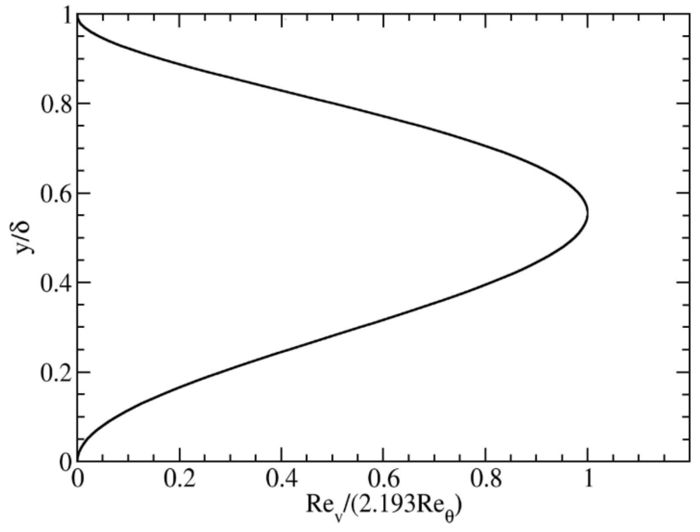

Scaled vorticity Reynolds number

Blending function from LM
To activate/inactivate terms outside the boundary-layer and wake-regions

Proposed Sensor Function: $S = S_1 \cdot F_{\theta t}$

Test Cases and Results

- Steady-State computations using Roe/HLLC upwind Scheme and the unfactored SSOR algorithm, along with use of low Mach preconditioning (when applicable)

- The predicted aerodynamic force coefficients have converged to five significant digits, the L2 norm of the residual for the flow equations has been reduced to 10^(−8) or lower

- Use of SST turbulence model with turbulence sustaining terms

- For automatic adaptation, the frequency of adaptation was set such that the L2 norm of the residuals for the mean flow and turbulence/transition model equations had also reduced to {10}^{-8} or lower

- Metrics for assessment: global force coefficients, C_p and C_f distributions, and how the results from the automatic adaptation approached those from equivalent universally refined grids

Fully Turbulent Flat Plate (SST-2003)

- Verification case from the NASA Turbulence Modeling Resource[1]
- $M_\infty = 0.2,\ Re/m = 5 \times 10^6, T_\infty = 300\text{K}$

Mesh Level	No. of points in the streamwise direction	No. of points in the wall-normal direction
Mesh 1	35	25
Mesh 2	69	49
Mesh 3	129	97
Mesh 4	257	193
Mesh 5	513	385

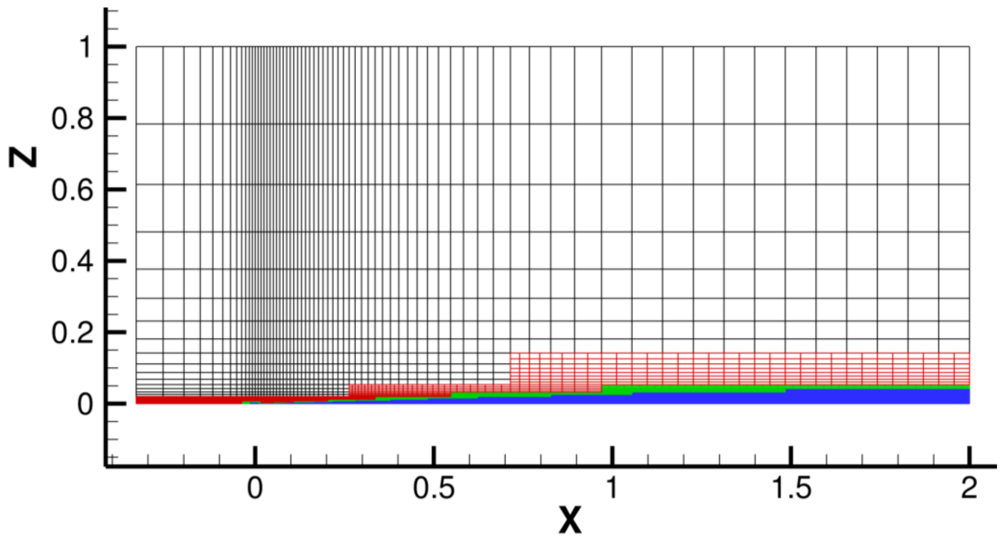

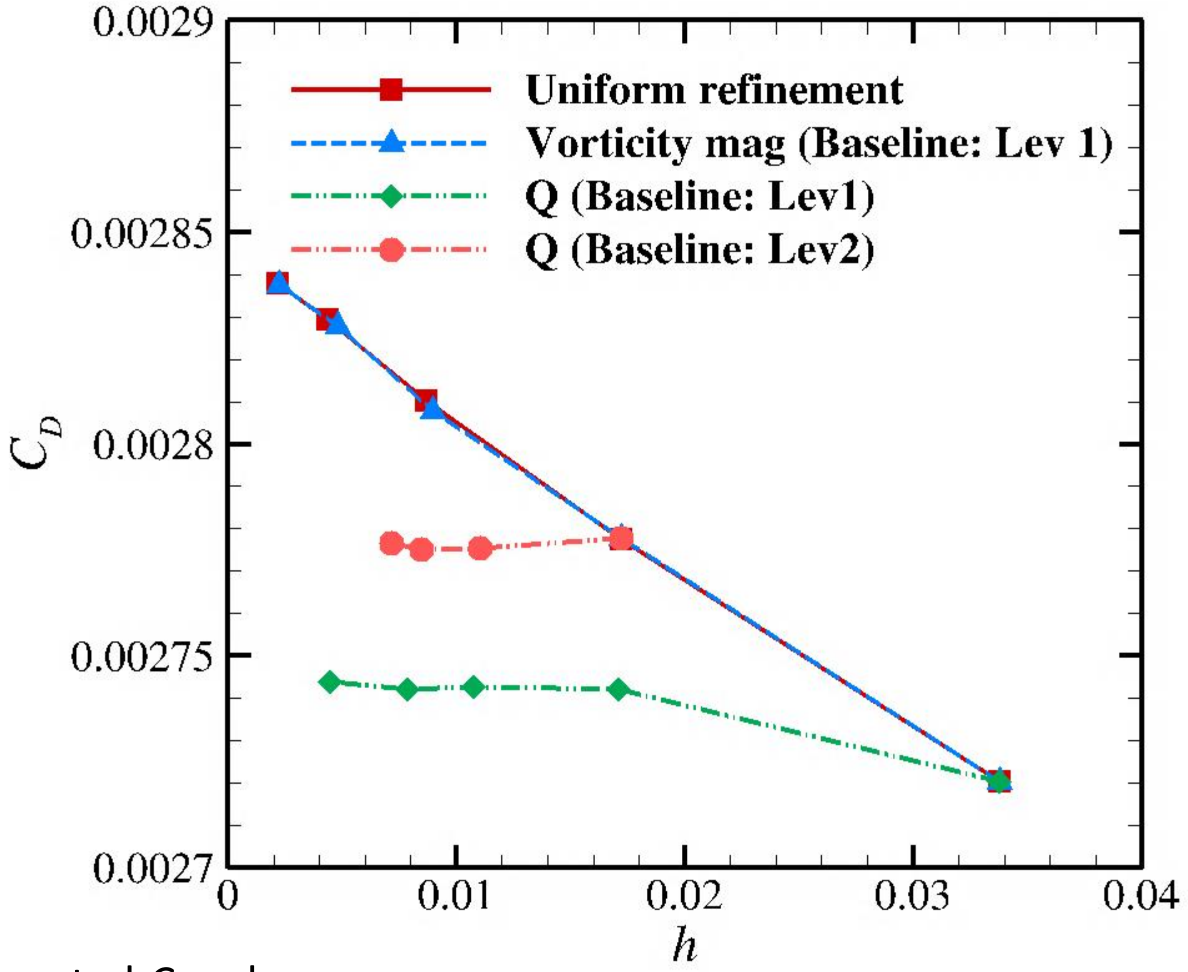

- Adapted mesh based on undivided Q did not converge to expected C_D values

1. https://turbmodels.larc.nasa.gov/

Flat Plate (Natural Transition)

- Experiment by Schubauer and Skramstad[1]
- $M_\infty = 0.147, \frac{Re}{m} = 3.36 \times 10^6, T_\infty = 288.17\text{K}$, Tu = 0.1337% and $(\mu_t/\mu)_{\text{inlet}}$ = 1.0
- Meshes doubled in number of points with alternative levels
- Baseline mesh level 5 had $y^+ \approx 0.25$ (turbulent flat plate estimate at the transition location: near wall spacing 4×10^{-6} m)

Mesh Level	No. of points in the streamwise direction	No. of points in the wall-normal direction	Points upstream of the leading edge
Mesh 1	181	97	49
Mesh 2	241	129	65
Mesh 3	361	193	97
Mesh 4	481	257	129
Mesh 9	2881	1537	769
Mesh 10	3841	2049	1025

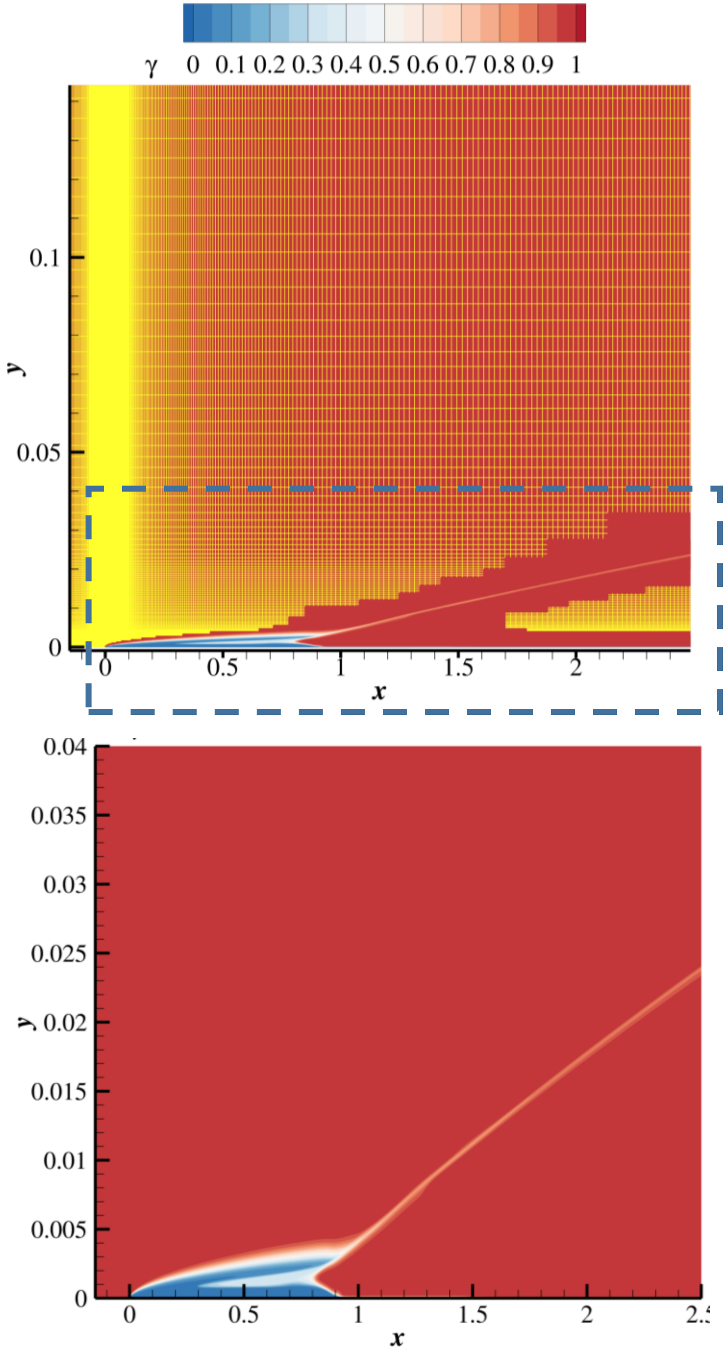

1. Schubauer, G. B., and Skramstad, H. K., "Laminar Boundary Layer Oscillations and Stability of Laminar Flow," *J. Aero. Sci.*, Vol. 14, No. 2, 1947, pp. 69–78.

Flat Plate (Natural Transition)

- Experiment by Schubauer and Skramstad[1]
- $M_\infty = 0.147, \frac{Re}{m} = 3.36 \times 10^6, T_\infty = 288.17\text{K}, Tu = 0.1337\%$ and $(\mu_t/\mu)_{\text{inlet}} = 1.0$
- Meshes doubled in number of points with alternative levels
- Baseline mesh level 5 had $y^+ \approx 0.25$ (turbulent flat plate estimate at the transition location: near wall spacing 4×10^{-6} m)

Mesh Level	No. of points in the streamwise direction	No. of points in the wall-normal direction	Points upstream of the leading edge
Mesh 1	181	97	49
Mesh 2	241	129	65
Mesh 3	361	193	97
Mesh 4	481	257	129
Mesh 9	2881	1537	769
Mesh 10	3841	2049	1025

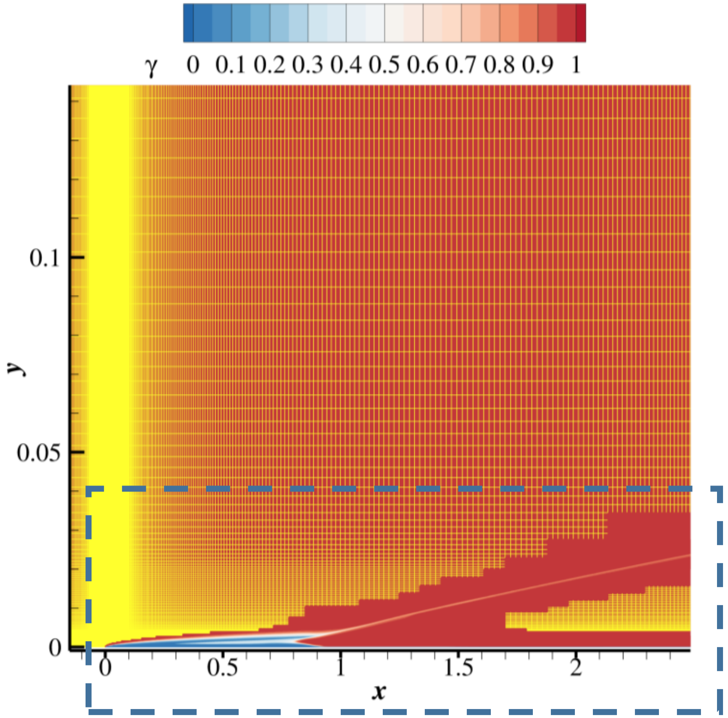

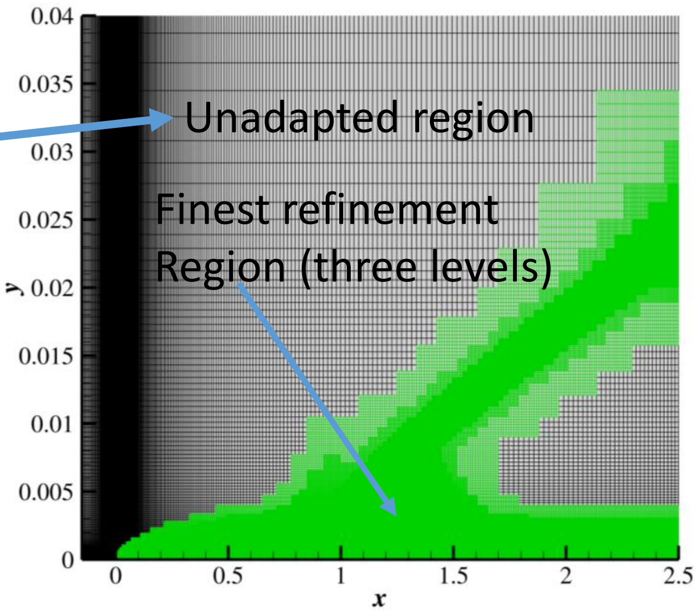

1. Schubauer, G. B., and Skramstad, H. K., "Laminar Boundary Layer Oscillations and Stability of Laminar Flow," *J. Aero. Sci.*, Vol. 14, No. 2, 1947, pp. 69–78.

Flat Plate (contd.)

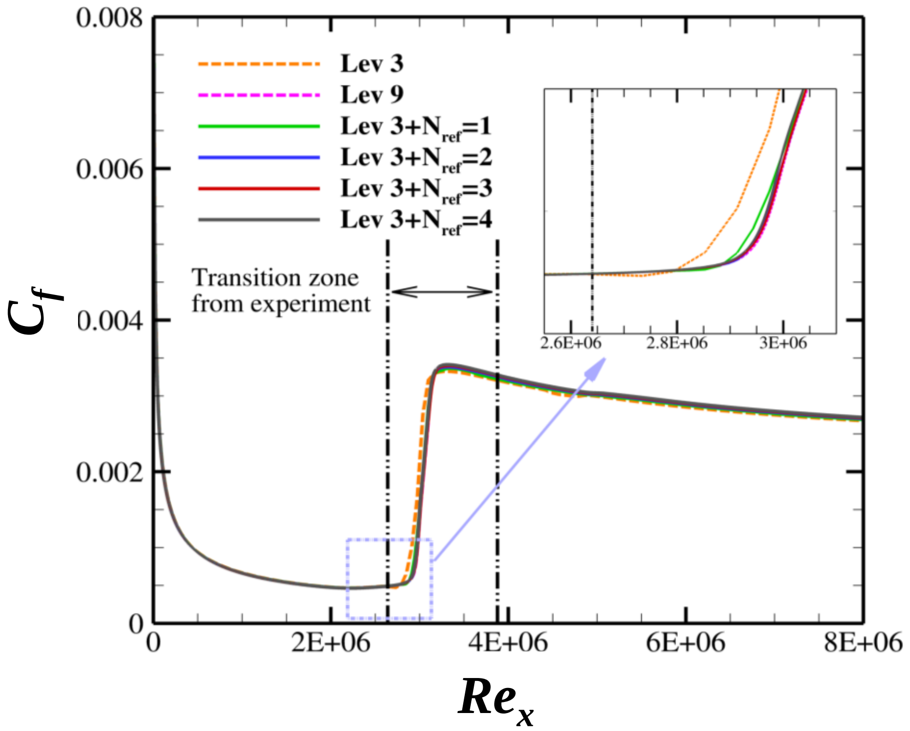

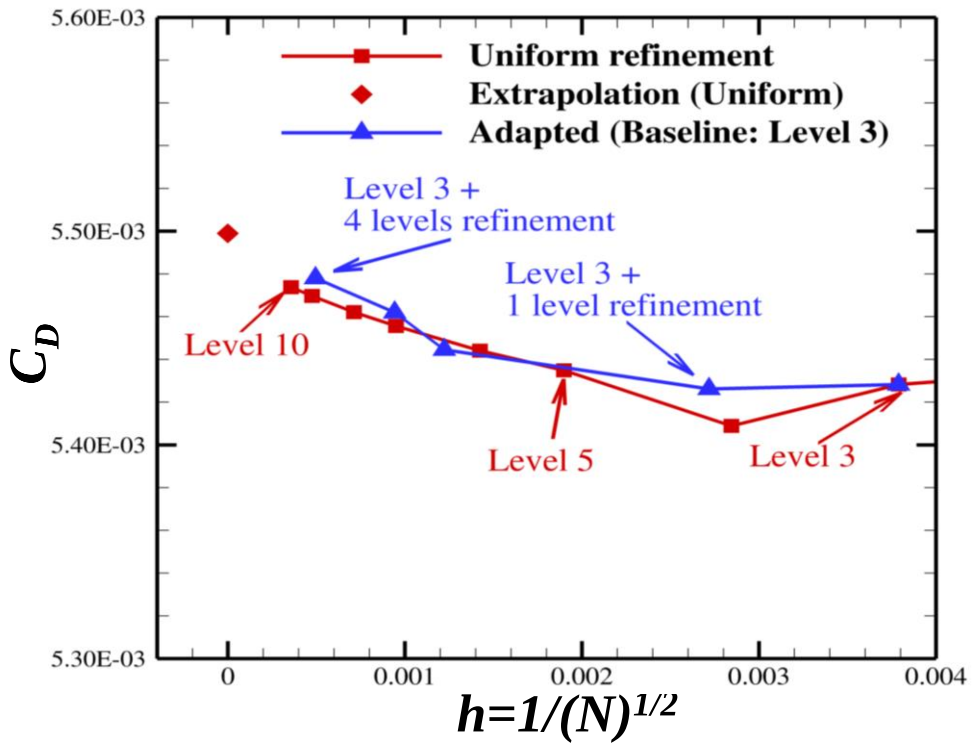

- Globally refined grids indicated convergence in C_f with mesh levels 3 and higher
    - Convergence in C_D needs grids of higher resolution
- Sensor adapted meshes approach convergence fewer degrees of freedom
    - Mesh level 3 + three levels of refinement had 75% fewer points than Mesh level 9
- Hildebrand et al. (2024): Wall normal resolution has a significant effect, even when streamwise grid is fine enough
- Isotropic adaptation $\Rightarrow$ Unable to discern the individual impact of wall-normal and streamwise resolutions

S809 Airfoil (Separation-induced transition)

- $M_\infty = 0.1, Re_c = 2.0 \times 10^6, T_\infty = 300\text{K}, \alpha = 1°, Tu = 0.07\%$, and $(\mu_t/\mu)_{inlet} = 1.0$
- C-grid topology; Outer boundary at 1000 chords
- Half the wall-normal points within one boundary-layer thickness
- Baseline mesh level 4 had $y^+ \approx 0.1$ (turbulent flat plate estimate at mid-chord: near wall spacing 1.15×10^{-6} chord length)
    - Used to create the coarser grids
- Good match obtained with finest adapted grids and globally refined grids (level 3/ level 4 meshes)

Mesh Level	S809		
	$N_x(N_{wake})$	N_y	N_{total}
Mesh 1	353 (49)	49	17297
Mesh 2	705 (97)	97	68385
Mesh 3	1409 (193)	193	271937
Mesh 4	2817 (385)	385	1084545

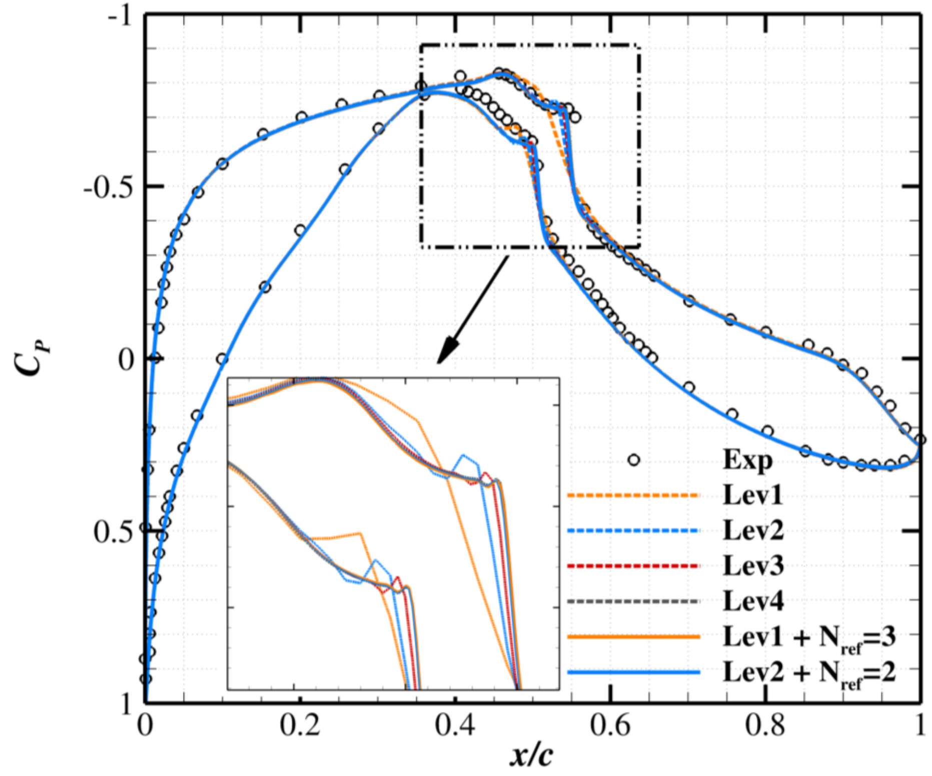

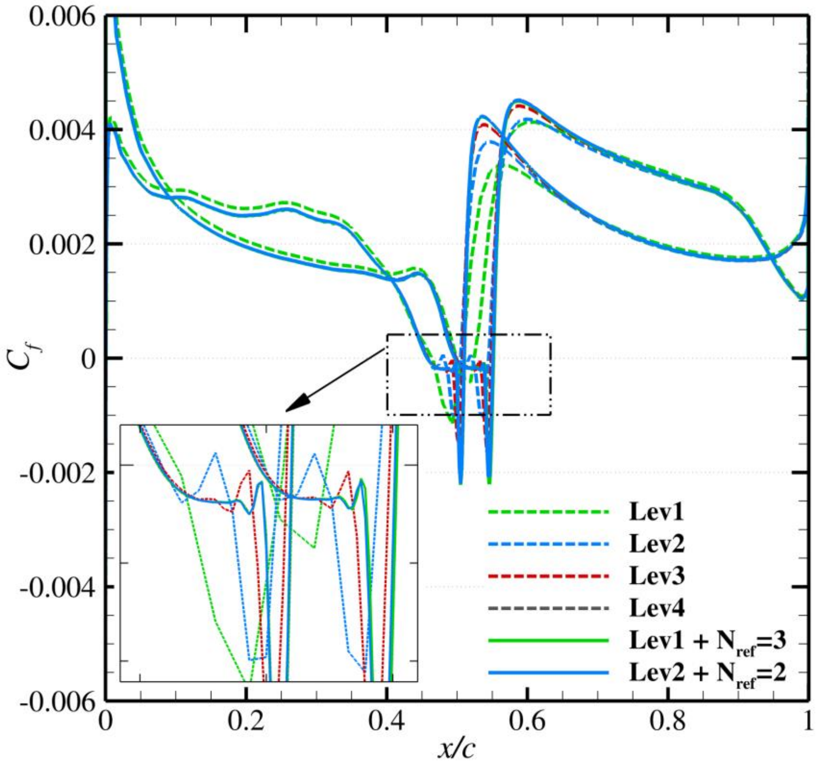

S809 Airfoil

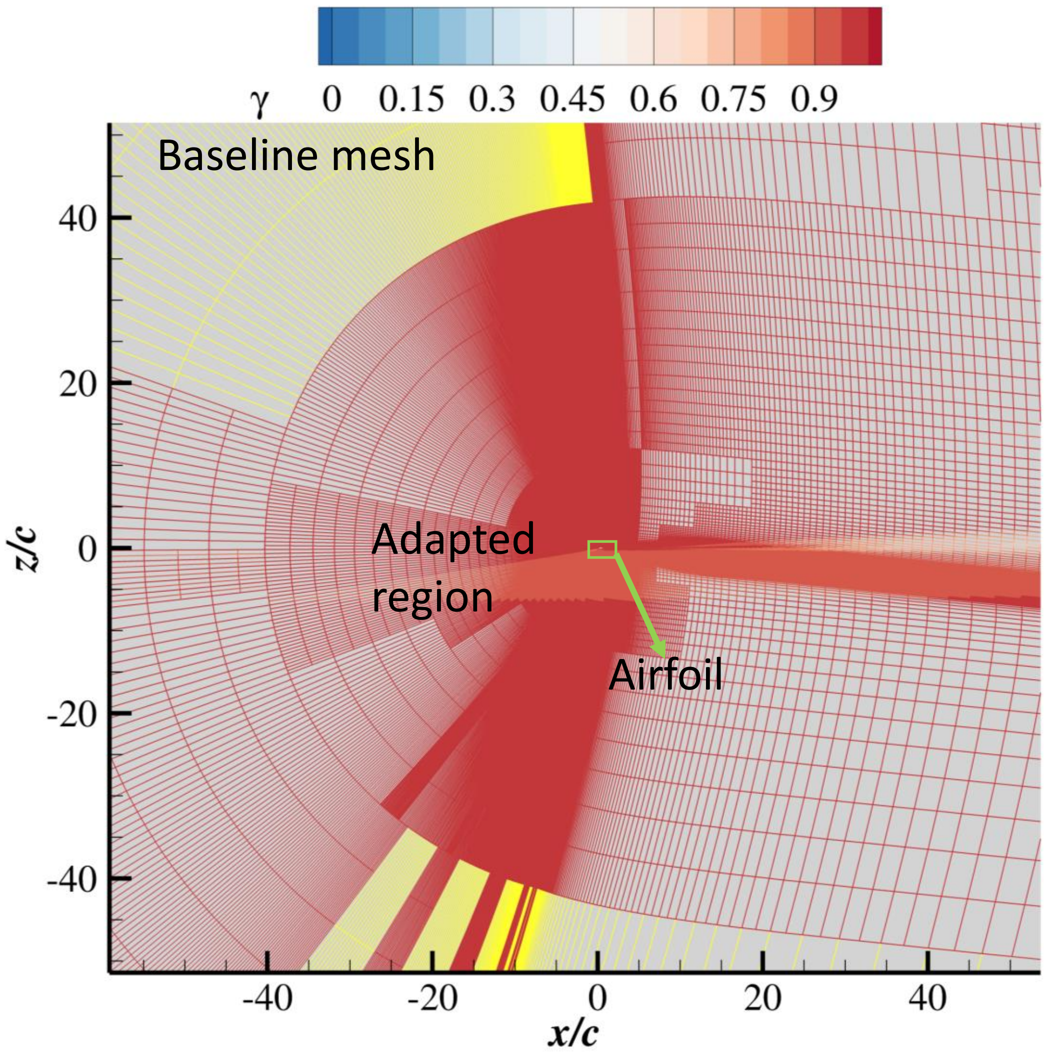

Baseline mesh level 2 + two levels of refinement

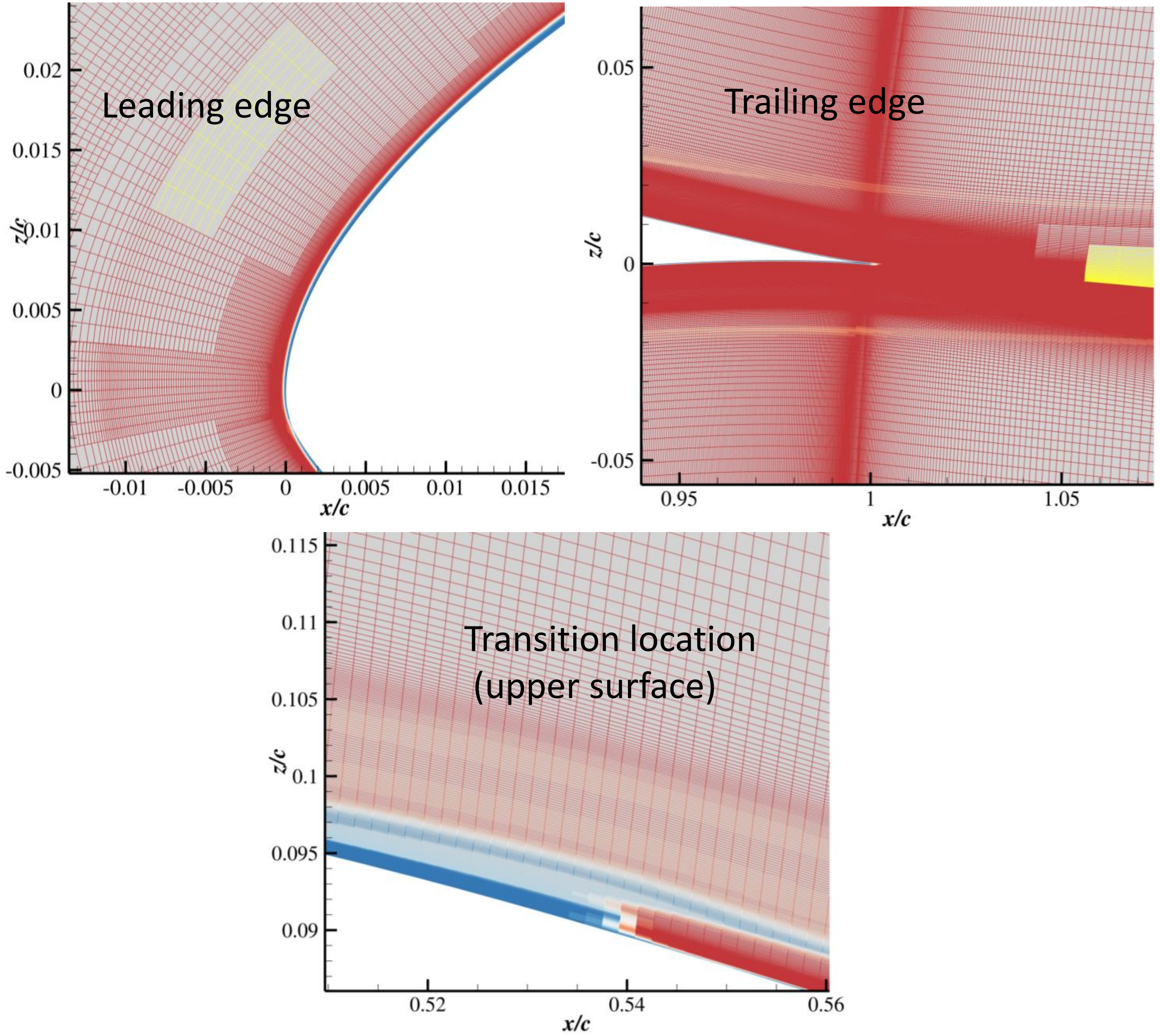

S809 (contd.)

Baseline mesh level	Grid Count	Baseline Mesh level 1	Adapted Grid Count	Savings (%)	Baseline Mesh level 2	Adapted Grid Count	Savings (%)
1	17,297	N_{ref} =0	17297	0.000			
2	68,385	N_{ref} =1	69702	-1.926	N_{ref} =0	68,385	0.000
3	271,937	N_{ref} =2	237387	12.705	N_{ref} =1	232,809	14.389
4	1,084,545	N_{ref} =3	821514	24.253	N_{ref} =2	898,845	17.122

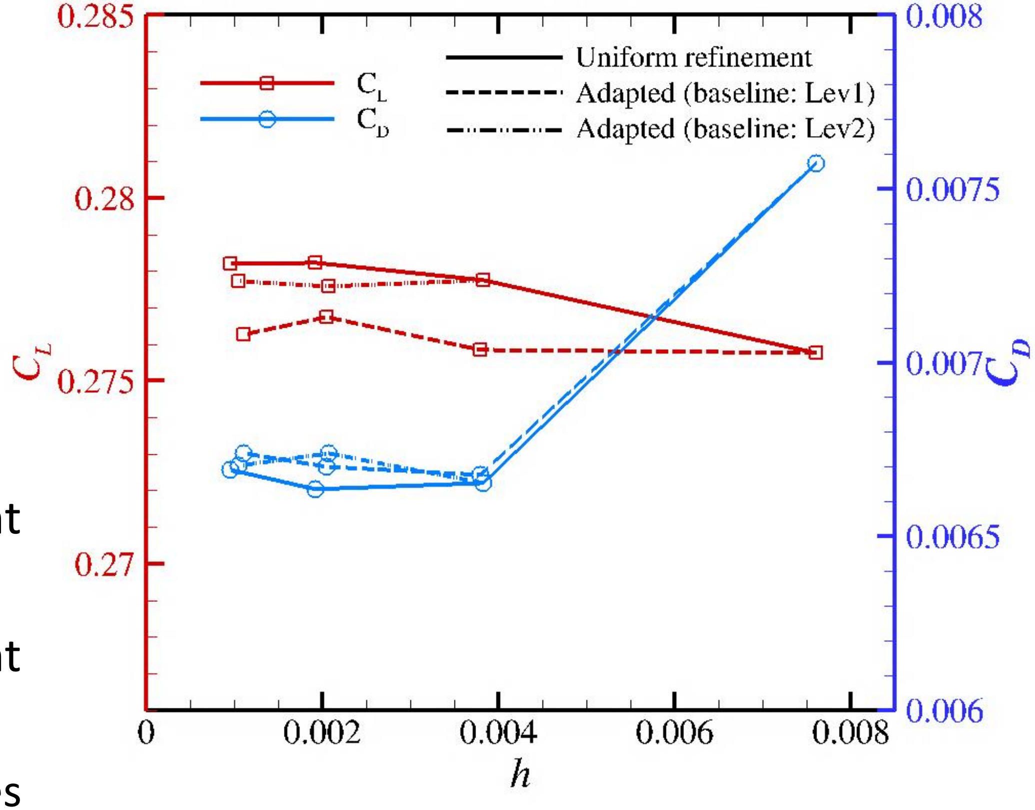

- Only modest savings in grid count; Minimum two levels of refinement needed
- Forces appear to be converging with global uniform refinement (additional grids needed to establish asymptotic convergence)
- When adaptation started from baseline meshes 1 or 2, drag approaches the reference values from finest globally refined grid
- Lift coefficient does not converge for adapted meshes started from baseline level 1 mesh (lower than reference value)
  - Parametric cubic interpolation to generate newer grid system relies on geometry from baseline mesh
  - Unfaithful geometric representation of regions with sharp changes in curvature

NLR-7301 Airfoil (Transonic)

- $M_\infty = 0.748, Re_c = 2.2 \times 10^6, T_\infty = 300\text{K}, \alpha = -2.267°, Tu = 0.158\%$, and $(\mu_t/\mu)_{inlet} = 1.0$
- Baseline mesh level 4 had $y^+ \approx 0.0625$ (turbulent flat plate estimate at mid-chord: near wall spacing 0.62×10^{-6} chord length)
  - O-grid topology
  - 600 points within one boundary-layer thickness (49 points in TE)

Mesh Level	S809		
	N_x	N_y	N_{total}
Mesh 1	307	169	51,883
Mesh 2	613	337	206,581
Mesh 3	1225	673	824,425
Mesh 4	2449	1345	3,293,905

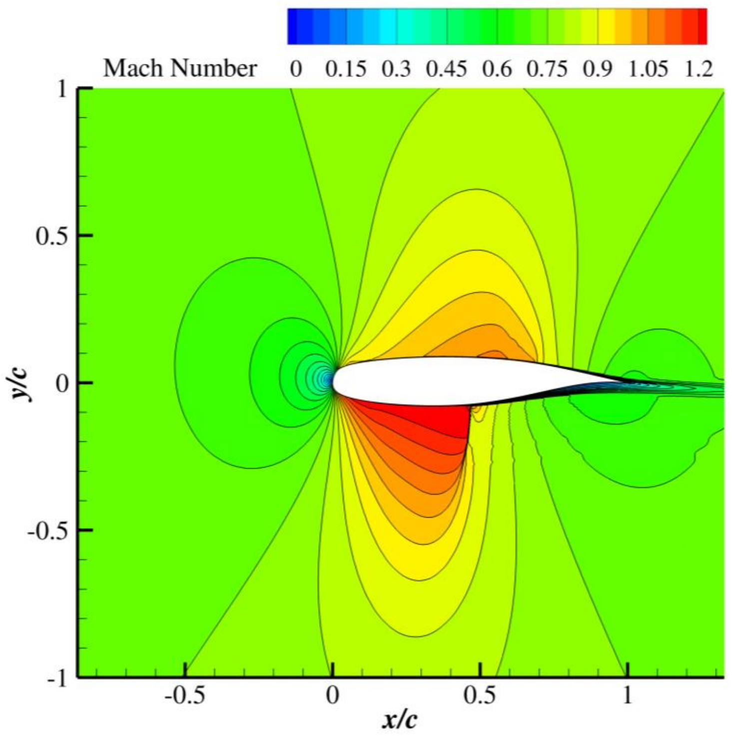

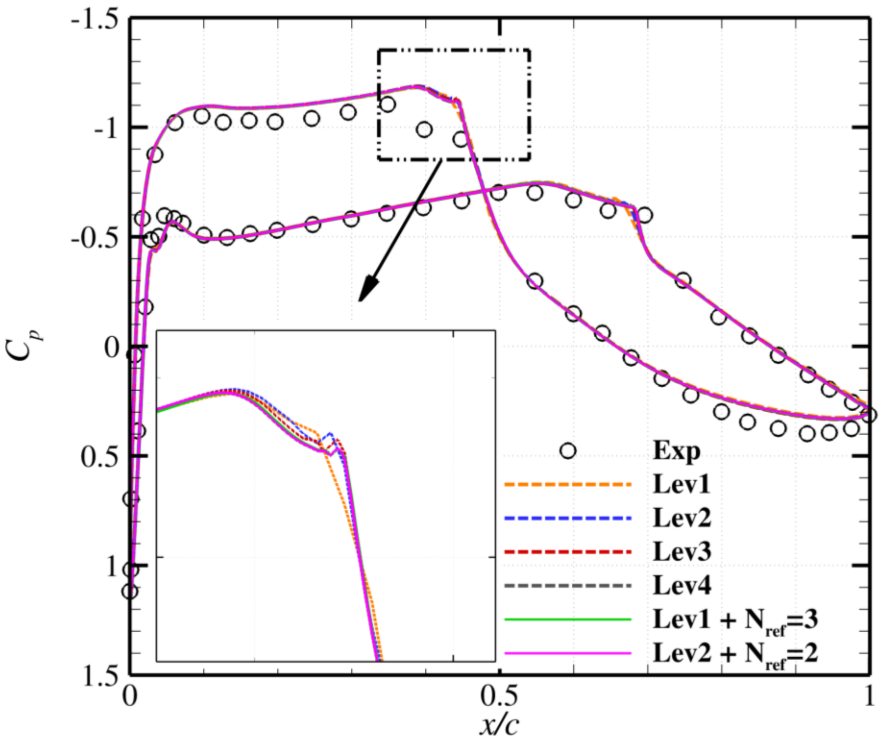

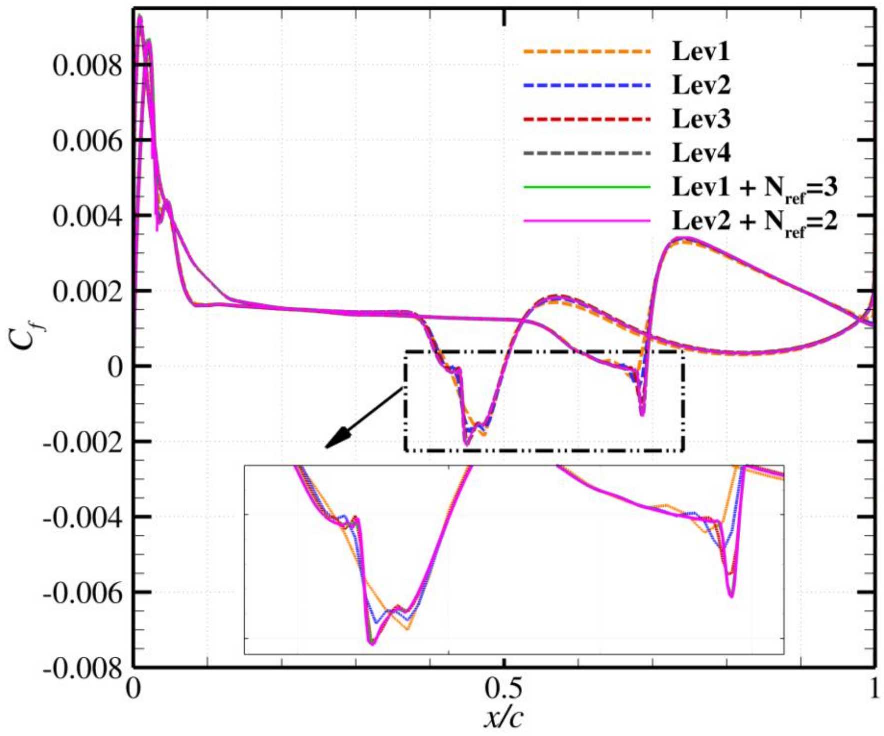

NLR-7301 Airfoil

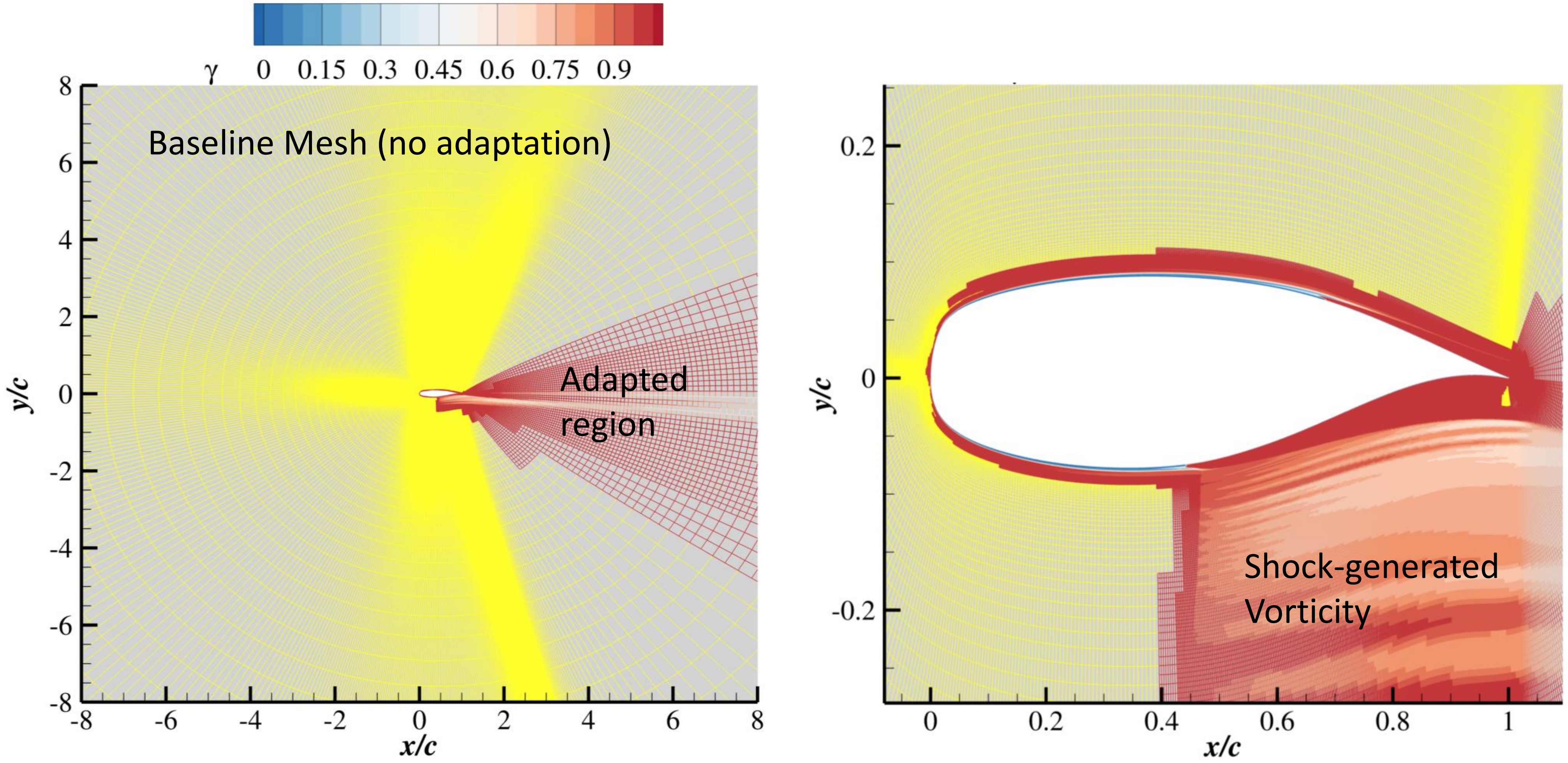

Baseline mesh level 2 + two levels of refinement

NLR-7301 Airfoil

Baseline mesh level	Grid Count	Baseline Mesh level 1	Adapted Grid Count	Savings (%)	Baseline Mesh level 2	Adapted Grid Count	Savings (%)
1	51,883	N_{ref} =0	51,883	0.000			
2	206,581	N_{ref} =1	175,398	15.09	N_{ref} =0	206,581	0.000
3	824,425	N_{ref} =2	593,845	27.97	N_{ref} =1	602,721	26.89
4	3,293,905	N_{ref} =3	2,127,232	35.42	N_{ref} =2	2,056,801	37.56

- Increased savings in grid count
  - Better wall-normal resolution
  - Refinement regions restricted around boundary layer
  - Sensor could be modified to handle shocks
- When adaptation is started from baseline mesh level 2, computed forces are closer the reference values from finest globally refined grid
- Additional refinement (globally refined and adapted grids) is necessary to check for the asymptotic convergence

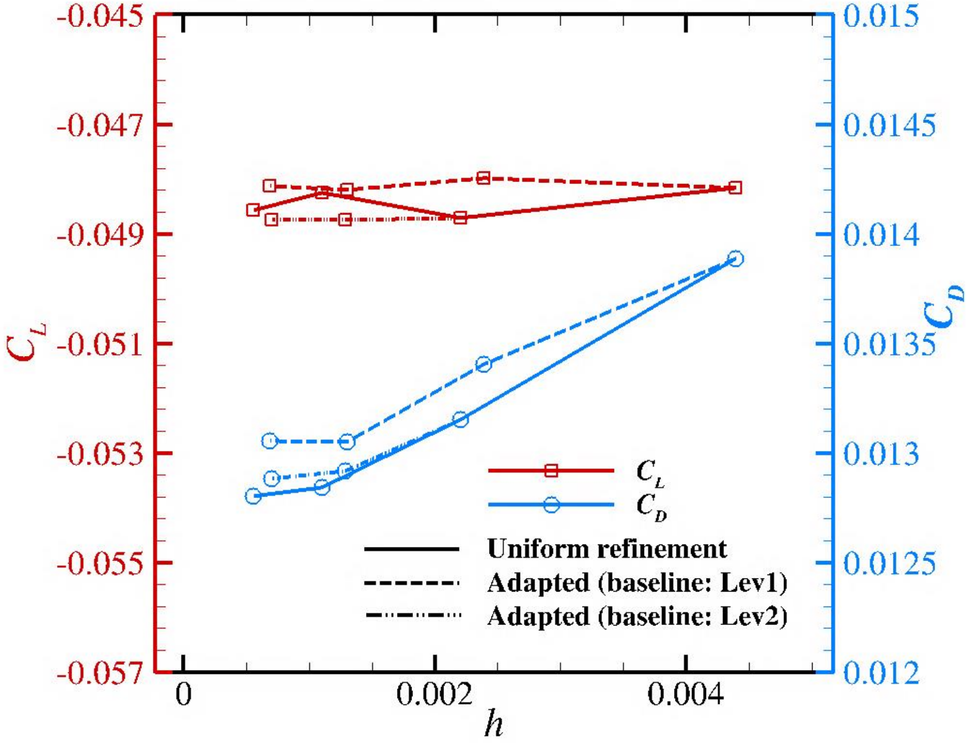

Summary

- Use of automated near-body mesh adaptation capability in OVERFLOW for achieving grid-insensitive solutions with reduced mesh counts with the Langtry-Menter model was explored
- An error sensor based on the undivided difference of the vorticity magnitude was evaluated using 2D canonical configurations (flat plate, S809, and NLR 7301 airfoils)
- Sensor was able to both identify critical regions of the flow and help accelerate solutions toward that from globally refined grids at a reduced cost
  - **For both airfoils, automatic adaptation was cost effective only when the starting baseline meshes were at level 2 or higher ⇒ Need for a minimum threshold resolution level for the baseline mesh used to begin the adaptation cycles**
  - **The savings in grid count achieved with the adaptation process, are neither negligible nor adequate (<35%),** and much smaller than those reported by Hildebrand et al. (≥ 3x) – **Shortcoming of isotropic adaptation**
- The isotropic adaptation process makes it difficult to discern if the streamwise or the wall-normal resolution is constraining the solution accuracy in a given region of the flow

Future Work

- Additional refinement (followed by Richardson extrapolation analysis) is necessary to provide a definitive benchmark for assessing the efficacy of the grid adaptation process in OVERFLOW
- The ability to perform anisotropic adaptation is expected to facilitate further reduction in the overall grid count, and hence, in the cost of model verification studies

Acknowledgments

- Research Funded by: NASA Transformational Tools and Technologies (TTT) Project
- The first author was supported by the NASA LaRC Research, Science, and Engineering Services (RSES) contract with Analytical Mechanics Associates.
- Dr. Pieter Buning at NASA LaRC for valuable insights through the course of this project
- LaRC K-Midrange Cluster resources

Thank You! Questions?

Backup Slides

S809 Airfoil

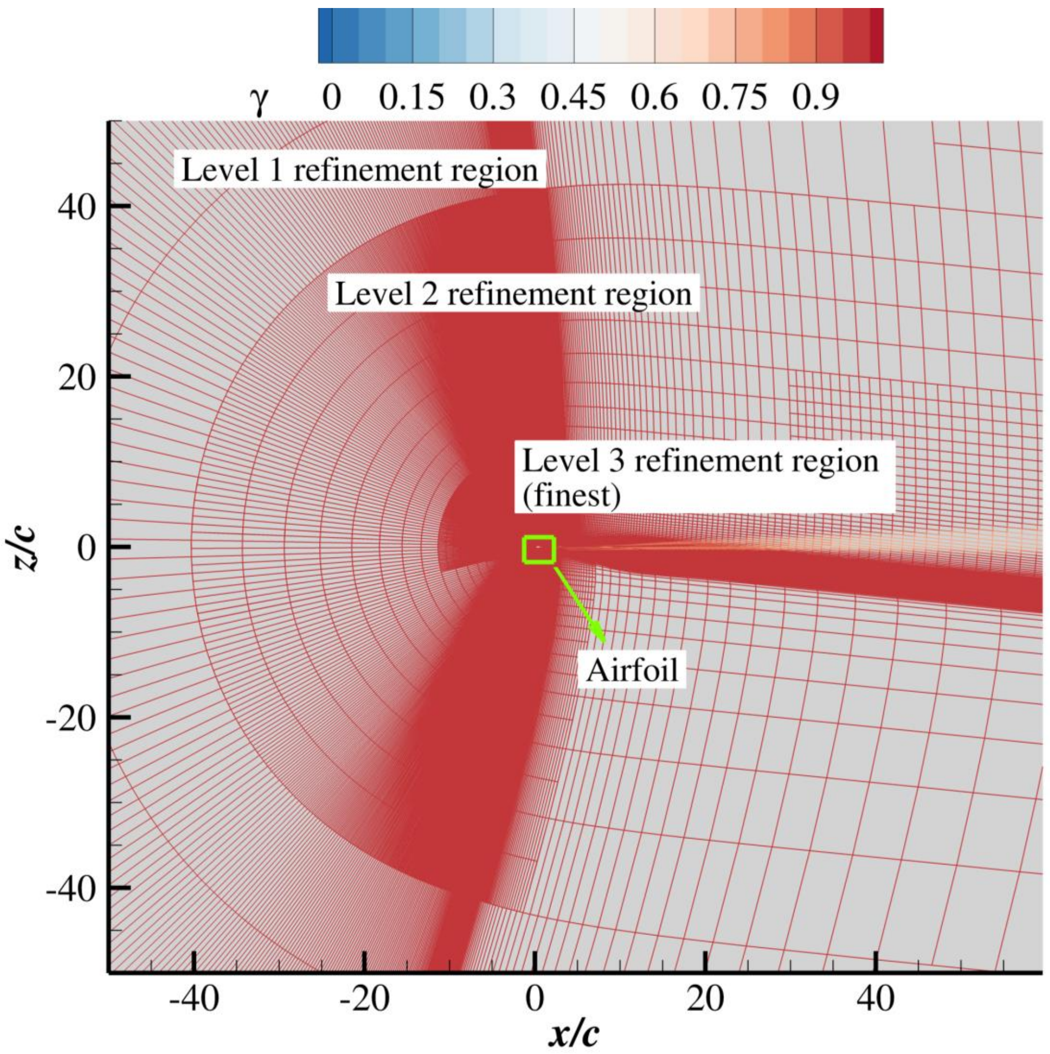

Baseline mesh level 1 + three levels of refinement

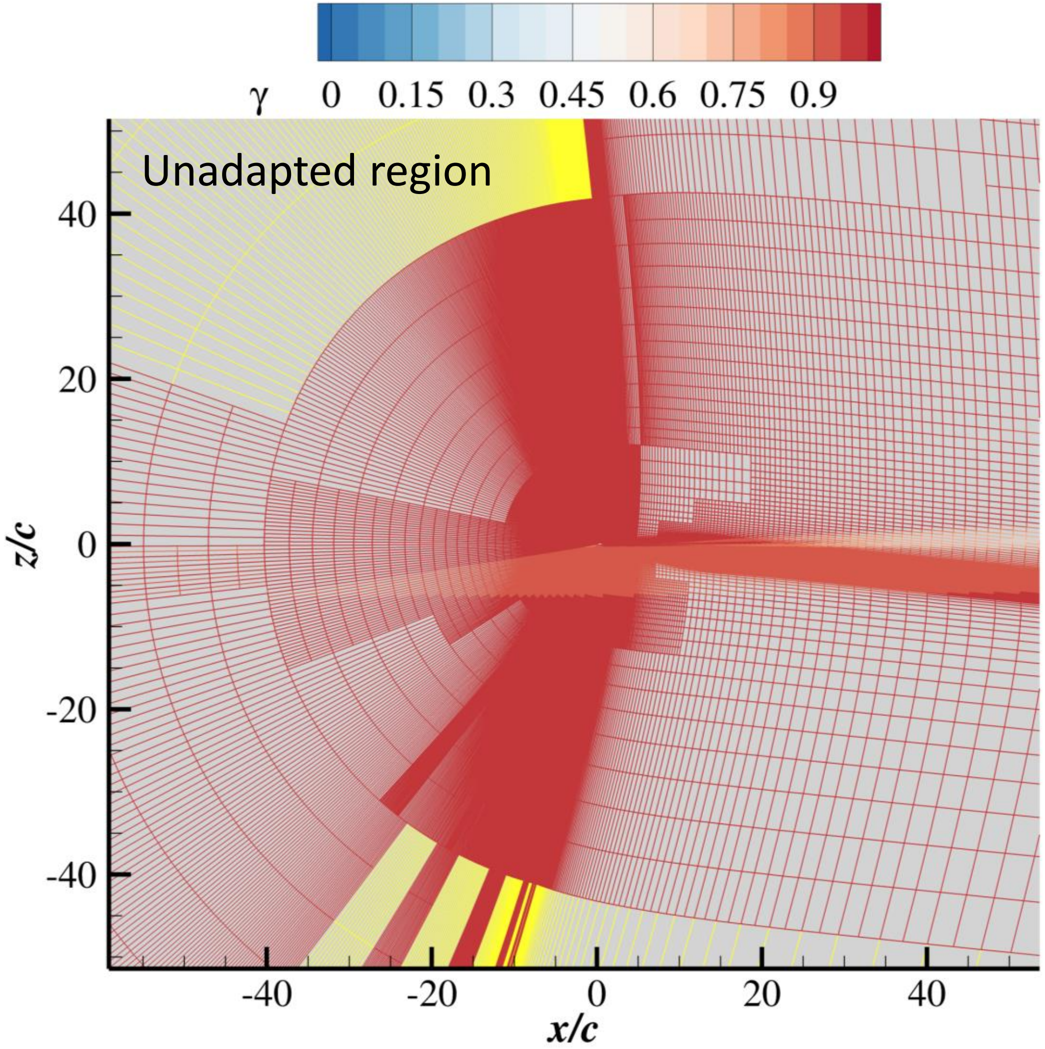

Baseline mesh level 2 + two levels of refinement

NLR-7301 Airfoil

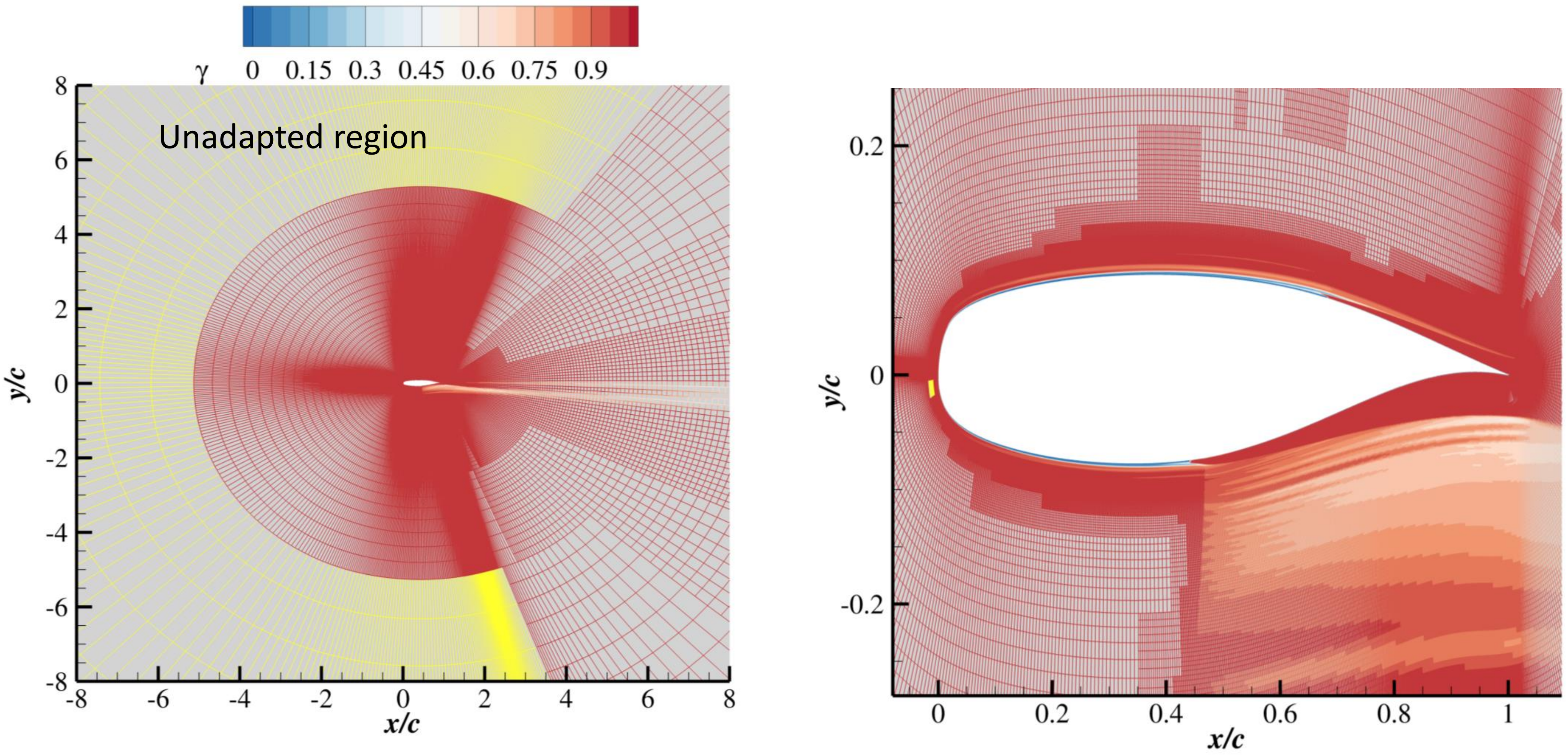

Baseline mesh level 1 + three levels of refinement